[5] Zung, L. and Breen, B. P., "Hypergolic Impingement Mechanism and Criteria for Jet Mixing or Separation," presented at the Sixth ICRPG Combustion Conference, CPIA Publication 192, Dec. 1969.

[6] Valentine, R. S., Rossi, F. S., and Kromrey, R. V., "Fluid Dynamic Effects on Apollo Engine Pressure Spikes," *Journal of Spacecraft and Rockets*, Vol. 5, No. 1, Jan. 1968, pp. 31–35.

[7] Houseman, J., "Combustion Effects in Sprays," presented at the Fifth ICRPG Combustion Conference, CPIA Publication 183, Dec. 1968.

[8] Kushida, R. and Houseman, J., "Criteria for Separation of Impinging Streams of Hypergolic Propellants," TM 33-395, July 1968, Jet Propulsion Lab., Pasadena, Calif.

[9] Landau, L. D. and Liftshitz, *Fluid Mechanics*, Addison-Wesley, Reading, Pa., 1959.

[10] Williams, F. A., "Detonations in Dilute Sprays," *ARS, Progress in Astronautics and Rocketry; Detonation and Two-Phase Flow*, Vol. 6, edited by S. S. Penner and F. A. Williams, Academic Press, New York, 1962, pp. 99–114.

[11] Houseman, J., "Optimum Mixing of Hypergolic Propellants in an Unlike Doublet Injector Element," *AIAA Journal*, Vol. 8, No. 3, March 1970, pp. 597–599.

[12] McLain, W. H. and Ross, L. W., "A Mechanism for the Initiation and Detonation in Hydrazine/Nitrogen Tetroxide Pulse-Mode Engine Residues," Paper 70-24, 1970 Fall Meeting, Western States Section, The Combusion Inst.

[13] Zung, L. B. and White, J. R., "Combustion Process of Impinging Hypergolic Propellants," Dynamic Science Rept. NAS 3-12031, 1971, NASA.

SEPTEMBER 1972 J. SPACECRAFT VOL. 9, NO. 9

Analytical Model of the Flash Produced in Aluminum-Aluminum Hypervelocity Impacts

KENNETH E. HARWELL,* KYNRIC M. PELL,† AND T. DWAYNE MCCAY‡

Auburn University, Auburn, Ala.

A theoretical model was developed which represents hypervelocity impact flash as radiation emitted from a high-temperature, optically thin, metallic plasma in local thermodynamic equilibrium. The model employs fundamental physical relationships to arrive at the radiation emitted from an impact plasma. Calculations were carried out for single element (pure aluminum) and multielement metallic plasmas. Two five-element plasma models were used to calculate radiation from type 2024 and type 6061 aluminum alloy impact plasmas. Calculations were carried out for the pressure of 1.0–100 atm and for temperatures of 5000 °K–40,000 °K. The theoretical results indicate that for these pressures and temperatures, the predominant type of radiation is that of spectral-line radiation. In order to obtain qualitative agreement between theory and experiment, it was necessary to include both impurity radiation effects and line shift-line broadening effects. This paper demonstrates that the flash emitted by a transient impact gas cloud can be represented as radiation from a high-pressure metallic plasma.

Introduction

EXPERIMENTAL studies[1–4] have indicated that the radiation emitted from a hypervelocity impact can be used to predict physical parameters associated with the projectile and target materials and to predict physical damage to the target. From only a knowledge of the impact flash, information on projectile mass, velocity,[4] and impact energy can be obtained. In an attempt to correlate the measured impact flash with the physical phenomena present in an impact event, the radiated energy is assumed to arise from high-temperature metallic gas at the projectile-target interface as shown schematically in Fig. 1. At the high temperatures expected, the hot gas will be in the plasma state. This physical model was adopted in order to predict the total radiation emitted from a unit volume of plasma in local thermodynamic equilibrium containing neutral atoms, ions, and electrons. By employing a fundamental approach to the calculation of the radiation, detailed knowledge of the spectral distribution of energy as a function wavelength and impact energy (or temperature of the impact plasma) can be obtained. This model permits quantitative calculations to be made for each of the radiation mechanisms. Such knowledge can assist in the design of diagnostic devices to measure impact flash. It also can assist in the design of devices to enhance radiation (e.g., illumination devices) and to reduce radiation (e.g., radiation and ionization in re-entry devices). Because the fundamental physical model is a general one, the mathematical equations can be applied to many practical situations.

Harwell, Reid, and Hughes[1] made an analytical study of an iron and aluminum plasma and found that such a representation

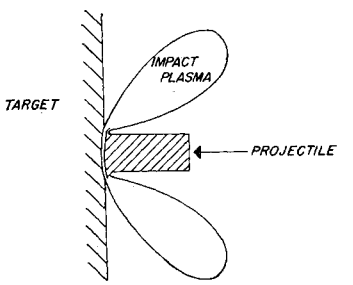

Fig. 1 Schematic representation of an impact plasma.

Received March 5, 1971; revision received April 14, 1972. This research was supported in part by the Air Force Armament Laboratory, Air Force Systems Command, Eglin Air Force Base, Fla., under contract F 08635-68-C-0033.

Index categories: Radiation and Radiative Heat Transfer; Hypervelocity Impact; Atmospheric, Space, and Oceanographic Sciences.

* Professor, Aerospace Engineering Department. Member AIAA.

† Assistant Professor, Aerospace Engineering Department; presently at University of Wyoming. Member AIAA.

‡ Graduate Assistant, Aerospace Engineering Department.

of impact flash as radiation from a high-temperature, high-pressure plasma appeared feasible. They found some qualitative agreement between theory and experiment for stainless steel impacts. However, there was a notable lack of agreement between theory and experiment for the aluminum impact events. The authors indicated that qualitative agreement between the theoretical calculations and the experimental measurements might be achieved by inferring line shift and line broadening, which were neglected in their model. In addition, they postulated that better agreement might be achieved if the model included more elements and more ions of each element. Their model included only two elements (iron and aluminum): three ions of aluminum and two ions of iron.

This article describes a theoretical study of the analytical model suggested by Harwell, Reid, and Hughes[1] and its extension to include radiation from multielement aluminum-alloy metallic plasmas and to include the effects of line shift and line broadening. The results of the calculations are compared with the experimental results presented by Harwell, Reid, and Hughes.[1]

Theoretical Considerations

Introduction to Theoretical Model

The theoretical model developed in this paper assumes that the radiation emitted during a hypervelocity impact event arises from a plasma created at the projectile-target interface. The radiation is assumed to arise from a unit volume containing neutral atoms, heavy positive ions, and electrons in local thermodynamic equilibrium (LTE). The latter assumption is made in order to simplify the theoretical model. In the actual impact event, the plasma created during the impact will be a highly transient one with spatial gradients in temperature, pressure, and composition. The radiating plasma will probably be a nonequilibrium one because of the rapid expansion of radiating gas from the point of impact. A complete analysis of such a nonequilibrium plasma would require a detailed knowledge of the specific physical mechanisms and collisions occurring in the radiating volume.

In addition, the quantitative calculation of the nonequilibrium radiation would require quantitative ionization rate and collisional cross section data. Lacking such data for nonequilibrium, high-pressure metallic plasmas, it was decided, as a first approximation, that the actual nonequilibrium event would be described as a succession of LTE states. Thus, although the plasma density and temperature may vary in space and time, the distribution of particles between the various energy states at any instant of time and location in space may depend only on the local values of temperature, density, and chemical composition of the plasma. These properties are assumed known or measurable in the present model. The assumption of LTE permits considerable simplification of the governing physical conditions since the population densities can be determined from the equipartition energy law of statistical mechanics without a quantitative knowledge of the atomic cross sections. For this case, the population of bound energy levels within a given species is described by Maxwell-Boltzmann statistics and the Boltzmann equation. The relative total populations of successive states of ionization are given by the mass action or Saha equations.

As stated by Griem[5-6] and discussed by Harwell, Reid and Hughes,[1] for moderately dense plasmas ($N_e \gtrsim 10^{16}\text{cm}^{-3}$) at moderate temperatures ($T \lesssim 6 \times 10^4\,^\circ\text{K}$), the velocity distribution of free electrons is almost always Maxwellian, so that Maxwell-Boltzmann statistics can be used in the solution of the present problem since these two conditions are normally satisfied in the hypervelocity impact plasma case.

Even though there are considerable amounts of energy radiated from the plasma volume, it is assumed in the present LTE model that the distribution function responds instantaneously to any change in the plasma conditions. In addition, each collisional process occurs at the same rate as its inverse so that the principle of detailed balancing is satisfied. Another requirement of the present model is that the ions and atoms in the plasma do not diffuse into regions of significantly different electron temperature in the relaxation time required for their level populations to reach equilibrium.[7] For the electron number densities of interest in impact plasmas ($N_e \geq 10^{16}$ cm^{-3}), the electron equilibration times are considerably shorter than the time required for equilibration of the bound energy levels of the atoms and ions. As long as the collisional rates of energy transfer are much higher than the radiative rates of energy transfer, the present LTE plasma model should give reasonable estimates of the energy radiated from an optically thin impact plasma.

Since all types of emitted radiation depend on free electron, ion, and/or neutral atom number densities, the first step in developing a mathematical model of the impact flash is to derive equations which yield the plasma composition as a function of local temperature and pressure. Once the composition of the multielement plasma is known, the radiation emitted in the form of line radiation, recombination radiation, and bremsstrahlung can be calculated.

Impact Plasma Composition

A brief description of the method used for calculating the composition of a multielement plasma is given next. A complete discussion of the mathematical derivation of the governing equations for a two-element plasma has been given by Harwell, Reid, and Hughes.[1] This derivation is an extension of their two-element equations to the case of a multielement plasma.

For a multielement plasma, the heavy particle number density is given by

$$N_H = \sum_{j=1}^{j_{\max}} \sum_{i=0}^{i_{\max}(j)} N_i(j) \tag{1}$$

where $N_i(j)$ is the density of the ith ion of the jth element. $N_o(j)$ is the neutral atom density for the jth element; $j_{\max}$ corresponds to the maximum number of elements and $i_{\max}(j)$ corresponds to the highest possible stage of ionization of the jth element.

Charge neutrality in the plasma requires that the number density of electrons, N_e, be given by

$$N_e = \sum_{j=1}^{j_{\max}} \sum_{i=0}^{i_{\max}(j)} (i) N_i(j) \tag{2}$$

The number density of each of the species in the plasma can be found from the laws of mass action (Saha equations), which can be written in the form

$$N_i(j) N_e / N_{i-1}(j) = K_i(j) \tag{3}$$

for $j = 1,2,\ldots,j_{\max}$ and $i = 1,2,\ldots,i_{\max}(j)$. $K_i(j)$ is the mass-action coefficient for the ith ion of the jth element. The mass action coefficients are functions of temperature and pressure and are defined by the expressions

$$k_i(j) = 2(2\pi m_e kT/h^2)^{3/2}\, Q_i(j)/Q_{i-1}(j) \exp\{[-E_i(j,\infty) + E_{i-1}(j,\infty)]kT\} \tag{4}$$

$Q_i(j)$ is the partition function for the ith ion of the jth element, $E_i(j,\infty)$ is the ionization energy for the ith ion of the jth element, T is the temperature, k is Boltzmann's constant, h is Planck's constant, and m_e is the mass of an electron.

Using Eq. (3), expressions for the number densities can be written as

$$N_i(j) = \frac{N_o(j)}{N_e{}^i} \prod_{r=1}^{i} K_r(j) \tag{5}$$

By combining the mass action Eqs. (3) with Eqs. (1) and (2), the total number of particles can be given as

$$N_T = N_H + N_e \tag{6}$$

or

$$N_T = \sum_{j=1}^{j_{max}} \sum_{i=0}^{i_{max}(j)} N_o(j) \frac{(1+i)}{N_e{}^i} \prod_{r=1}^{i} K_r(j) \tag{7}$$

If the number density defined by Eq. (5) is summed over all the ions for a particular element, the result is the total number density of particles for that element, i.e.,

$$N_H(j) = \sum_{i=0}^{i_{max}(j)} N_i(j) \tag{8}$$

This result can be rewritten in terms of the number of atoms in the neutral state by using Eq. (5) as

$$N_H(j) = N_o(j) \sum_{i=0}^{i_{max}(j)} \frac{1}{N_e{}^i} \prod_{r=1}^{i} K_r(j) \tag{9}$$

Thus the expression for the total number of particles can be written as

$$N_T = \sum_{j=1}^{j_{max}} N_H(j) \sum_{i=0}^{i_{max}(j)} \frac{(1+i)}{N_e{}^i} \prod_{r=1}^{i} K_r(j) \Big/ \sum_{i=0}^{i_{max}(j)} \frac{1}{N_e{}^i} \prod_{r=1}^{i} K_r(j) \tag{10}$$

For convenience, define the relative amounts of heavy particles present in the plasma as the partial pressure of the jth element:

$$PP(j) = N_H(j)/N_H \tag{11}$$

The number of heavy particles present is just

$$N_H = N_T - N_e \tag{12}$$

Equations (11) and (12) can be used along with Eq. (10) to derive an electron density polynomial of the form

$$\frac{1}{1 - \dfrac{N_e}{N_T}} = \sum_{j=1}^{j_{max}} PP(j) \frac{\displaystyle\sum_{i=0}^{i_{max}(j)} \frac{(1+i)}{N_e{}^i} \prod_{r=1}^{i} K_r(j)}{\displaystyle\sum_{i=0}^{i_{max}(j)} \frac{1}{N_e{}^i} \prod_{r=1}^{i} K_r(j)} \tag{13}$$

For the metallic plasmas studied in this article, $PP(j)$ and N_T are assumed known. N_T is calculated using the equation of state in the present study and $K_r(j)$ is calculated as a function of temperature; $i_{max}(j)$ and j_{max} are assumed to be known in the present study, but $i_{max}(j)$ could be determined as a function of temperature. Thus, for given $PP(j)$, T, and N_T, Eq. (13) is essentially a complex polynominal of order

$$\sum i_{max}(j) + 1$$

in the unknown electron density. For example, for the case of five elements ($j_{max} = 5$) and five ions of each element ($i_{max}(j) = 5$), the polynomial would have five terms and be of the 25th order in the unknown electron density. However, because of the manner in which the terms are written, $N_e{}^5$ will be the highest power of the electron-density term.

As shown in Eq. (4), the mass action coefficients $K_i(j)$ are functions of the partition functions $Q_i(j)$ which are defined as

$$Q_i(j) = \sum_{n=1}^{n_{ci}(j)} g_i(j,n) \exp[-E_i(j,n)/kT] \tag{14}$$

for a gas obeying Maxwell-Boltzmann statistics; $g_i(j,n)$ is the statistical weight of the nth energy level $E_i(j,n)$ of the ith ion of the jth element. The partition function is summed theoretically for all values of the principal quantum number, n, between the lowest quantum number n_1, corresponding to the ground state energy level, and the so-called terminating or cut off quantum number, n_c, corresponding to the lowered ionization potential in a plasma.

One difficulty which arises in the evaluation of the partition function for a plasma is that the series in Eq. (14) must be truncated to include only those energy levels which are below the effective ionization potential. The effective ionization potential is somewhat below the ionization potential for an isolated atom because of the interaction of charged particles in a plasma. Electrons with energies higher than that corresponding to the maximum principal quantum number n_c are considered to be free electrons.

Using the Debye shielding criterion,[1,8,9] the series cutoff quantum number is found to be

$$n_{ci}(j) = 36.11 \times 10^3 [Z^2_{eff}(i,j)T/N_e + \sum_i \sum_j Z_i{}^2(j) N_i(j)]^{1/4} \tag{15}$$

Z_{eff} is the effective charge of an atom or ion as seen by an excited electron, and $Z_i(j)$ is the effective charge corresponding to the ith ion of element (j). The effective charge is assumed to be one for atoms, two for singly-charged atoms, etc. Implicit in Eq. (15) is the assumption that highly excited atoms and ions behave as hydrogenic atoms.

Since the cutoff quantum number is density-dependent, the calculation of n_c will be coupled to the iterative solution of the highly nonlinear set of mass action Eqs. (3), the electron density polynomial Eq. (13), and the partition function Eq. (14). The calculation procedure normally adopted is to assume a value of the cutoff quantum number with which to calculate initial partition functions and mass action coefficients. The electron density is then determined from a solution of the electron density polynomial (13). Heavy particle number densities are then calculated using the mass action Eqs.(3). A new cutoff quantum number is calculated, and the procedure continued until a convergent cutoff quantum number is determined. This iterative procedure yields the plasma composition for a given temperature and total number density of a known multielement gas.

During the course of the research study, it was found that the metallic elements could be classified as aluminumlike elements or ironlike elements. Aluminumlike elements are defined as those metals for which the energy levels can be classified simply in terms of the principal quantum numbers. For these elements, $N_{ci}(j)$ is determined using the iterative scheme described earlier. For the case of iron and ironlike elements which exhibit very complex spectra and are difficult to classify with respect to the principal quantum number, the cutoff quantum number is set equal to the quantum number of the highest observed energy level. For the ironlike elements, the cutoff quantum number does not change as a function of temperature and pressure. The partition function of the ironlike elements is then only a function of temperature. Consequently, the iterative loop on cutoff quantum number is not needed for the ironlike elements.

Radiation from an LTE Optically-Thin Plasma

The radiation emitted from a unit volume of optically thin plasma in local thermodynamic equilibrium is assumed to be one of the following types: 1) line emission because of internal (bound-bound) transitions in the atoms and ions, 2) continuum emission because of electron-ion recombination (free-bound) transition, and 3) continuum emission (bremsstrahlung) because of electron-ion collision (free-free) transitions.

Line Radiation

Line radiation can occur when electrons make transitions between bound energy levels of an atom or ion. Emission of energy in the form of a photon of energy

$$h\nu(m,n) = E_i(m) - E_i(n) \tag{16}$$

occurs when an electron makes a transition from a bound level of higher energy, $E_i(m)$, to one of lower energy, $E_i(n)$. ν is the frequency, m and n are the principal quantum numbers of the upper and lower energy levels, respectively, and $E_i(m)$ is the energy in level m for a particle of ionization stage i.

As shown by Harwell, Reid, and Hughes,[1] the total power

radiated per unit volume per unit solid angle in the line at the frequency ν is

$$P_{ij}{}^{L}(\nu) = \frac{h\nu}{4\pi}\frac{N_i(j)}{Q_i(j)} g_i(j,m)\, A_i(m,n) \exp[-E_i(j,m)/kT] \quad (17)$$

where $A_i(m,n)$ is the probability that a transition will occur from energy level m to energy level n.

It is well-known that because of the interactions which occur in a plasma between the emitting ions and atoms, the transitions will not occur at one precise energy or frequency, so that the energy in a given spectral line will be distributed about a given frequency (or wavelength). The spectral line is then said to be broadened and to possess a line shape or profile $L(\nu)$ such that the probability of emission in the frequency interval $d\nu$ is defined as $L(\nu)\, d\nu$. $L(\nu)$ is normalized such that $\int L(\nu)d\nu = 1$. The power radiated per unit volume per unit solid angle per frequency interval is

$$P_{ij}{}^{L}(\nu)d\nu = \frac{h\nu}{4\pi}\frac{N_i(j)}{Q_i(j)} g_i(j,m)A_i(m,n)\exp[-E_ij,m)/kT]L(\nu)d\nu \quad (18)$$

In addition to being broadened, the spectral line is shifted from the isolated atom wavelength. The effects of broadening and line shift will be discussed later.

Recombination Radiation

Recombination radiation is a form of continuum radiation where an electron recombines with an ion in a lower stage of ionization and a photon is emitted with energy

$$h\nu = E_i(j,\infty) - E_i(j,n) + \tfrac{1}{2}m_e v_e{}^2 \quad (19)$$

where v_e is the electron velocity and $E_i(j,n)$ is the bound state energy level of the recombined electron ion.

As described in considerable detail by Harwell, Reid, and Hughes,[1] by requiring a balance between recombination and ionization events in equilibrium, and relating the ionization cross sections to transition probabilities, the recombination radiation in the wavelength interval $d\lambda$ per unit volume of the radiating source per unit solid angle is found to be

$$P_{ij}{}^{R}(\lambda)d\lambda = \frac{16_e{}^4}{3\ 3\pi m_e{}^2c^2}\frac{Z_{\text{eff}}(i,j)}{\lambda^2} N_eN_i(j)\,[E_i(j,\infty)kT]\times$$
$$\exp(-hc/\lambda kT)\sum_{n_{\min(i,j)}}^{n_{ci(j)}}\frac{g_{fb}}{n^3}\exp\left[\frac{E_i(j,\infty)-E_i(j,n)}{kT}\right] \quad (20)$$

The g_{fb} is the free-bound Gaunt factor and $n_{\min}(i,j)$ is defined by

$$n^2{}_{\min}(i,j) = n_{ci}{}^2(j)\, E_i(j,\infty)[n_{ci}{}^2(j)h\nu + E_i(j,\infty)] \quad (21)$$

The sum in Eq. (20) is carried out over all bound states available to the recombining electron.

In the calculation of recombination radiation for this study, the free-bound Gaunt factor was assumed to be 1 . Eq. (20) was derived for the case of hydrogenic atoms and ions. For nonhydrogenic atoms (which is probably the case for most impact materials), the photoionization cross section must be evaluated. As indicated in Ref. 1, only very few cases have been considered even in an approximate theoretical way. There are relatively few reliable experiments to assist the theoretical development. Until additional theoretical and experimental information becomes available, this hydrogenic approximation for the continuum radiation should give at least a first estimate of the emitted power resulting from recombination radiation.

Bremsstrahlung

Bremsstrahlung results when an electron changes from one free-energy state $E(v_1)$ to another free energy state $E(v_2)$ with the emission of a photon of energy.

$$h\nu = E(v_1) - E(v_2) \quad (22)$$

Bremsstrahlung is caused by the deceleration of charged particles in the Coulomb field of other charged particles. The major contribution to this type of radiation for the plasmas studied in this report is that due to electron-ion collisions. Since there are an infinite number of initial and final states, the radiation spectrum is continuous.

As derived in Ref. 1, the bremsstrahlung contribution to the radiated power is given by

$$P_{ij}{}^{B}d\lambda = \frac{8_e{}^4h\nu}{3\ 3r\pi m_e{}^2c^2}\frac{Z_{\text{eff}}}{\lambda^2} N_eN_i(j)\,[E_i(j,\infty)/kT]^{1/2}\times$$
$$g_{\text{ff}}\exp[E_i(j,\infty)/n_{ci}{}^2(j)kT]\exp\left[-\frac{h\nu}{kT}\right]d\lambda \quad (23)$$

where g_{ff} is the free-free Gaunt factor which was assumed to be one for the present calculation. As was the case for the recombination radiation calculations, this expression was derived for the case of hydrogenic atoms and ions.

Spectral Line Broadening and Line Shift

Spectral lines have shapes and widths that depend on the environment of the emitting atom or ion in the plasma and are strongly dependent on the pressure and temperature. The broadening mechanisms which may be of importance in a plasma are natural broadening, Doppler broadening, and pressure broadening. Natural line broadening is the result of the finite lifetime of the excited states and is usually quite small. Doppler broadening is the result of the motion of the emitting atom or ion and is most pronounced for spectral lines of light elements at high temperatures and relatively low electron densities. When the line profiles are determined predominately by interactions of the emitting atoms or ions with the surrounding particles, the broadening is called pressure broadening. Pressure broadening may be subdivided into 1) resonance, 2) Van der Waals, and 3) Stark broadening, depending on whether the broadening is caused by interactions with 1) atoms of the same kind (one of the states of the line must interact with the ground state), 2) atoms or molecules of different kinds, or 3) charged particles. Broadening by neutrals is several orders of magnitude larger than that due to charged atoms. For high enough electron and ion concentrations (about 1% of the total density), the long range Coulomb forces are dominant and only Stark broadening need be considered.

Stark broadening can be calculated using the impact approximation and the quasi-static approximations.[6] A theoretical treatment developed by Griem and co-workers[6] that combines impact broadening to treat electron interactions with the quasi-static approximation to handle the ion interaction was used in these calculations. The result of this theory for the reduced profiles of allowed components is

$$j(x) = \frac{1}{\pi}\int_0^\infty \frac{d\beta W_r(\beta)}{1+(x-\alpha^{4/3}\beta^2)^2} \quad (24)$$

where $\alpha = (c_2F_0{}^2/w)^{3/4}$ and $x = (\lambda - \lambda_0 - d)/w\lambda$.

The asymptotic form (large x) of Eq. (24) is

$$j(x) \doteq 1/\pi x^2 + 3\alpha/4x^{7/4} \quad (25)$$

in the direction of the line shift and

$$j(x) \doteq 1/\pi x^2 \quad (26)$$

in the opposite direction.

Parameters which can be used for the determination of approximate line profiles of some heavier elements have been tabulated by Griem.[6] The profiles are determined primarily by electron broadening which results in an approximately Lorentzian shape, whereas the ionic contribution causes some

asymmetry in the profiles. For the cases where the following conditions are satisfied

$$\sigma = 8.0 \times 10^{-2} w/\lambda^2 (T/\mu) - {}^{1/2} N_e^{2/3} > 1$$

$$R = 9.0 \times 10^{-2} N_e^{1/6} T - {}^{1/2} < 0.8$$

$$10^{-4} N_e^{1/4} \alpha < 0.5$$

The total (half) half-width of atomic lines is approximately given by

$$\Delta\lambda_w = [1 + 1.75 \times 10^{-4} N_e^{1/4} \alpha (1 - 0.068 N_e^{1/6} T^{-1/2})] 10^{-16} w N_e \quad (27)$$

and the shift of the line is approximately

$$\Delta\lambda_s = [d/w \pm 2.0 \times 10^{-4} N_e^{1/4} \alpha (1 - 0.068 N_e^{1/6} T^{-1/2})] 10^{-16} w_n e \quad (28)$$

w is the electron impact (half) half-width (at $N_e = 10^{16}\text{cm}^{-3}$), λ is the wavelength in Å, α is the ion-broadening parameter, d is the shift resulting from electron impacts, and μ is the atomic weight. These formulas may also be applied to singly ionized atomic lines if the factor 0.068 is replaced by 0.11.

In order to develop a tractable computer program to handle Stark broadening, these shifts and widths were used in a Lorentzian line profile. The total radiated energy in the line was normalized to the unperturbed value, so that

$$I_{\text{unperturb}} = K \int_0^\infty \frac{\Delta\lambda_w \, d\lambda}{(\lambda - \lambda_0 - \Delta\lambda_s)^2 + (\Delta\lambda_w)^2} \quad (29)$$

where K is the normalization constant. The integral can be evaluated to yield a numerical result for K

$$K = I_{\text{unperturb}}/\pi \quad (30)$$

The contribution of each spectral line to the total radiation in a given spectral band is then given as

$$I_{\text{band}} = K \int_{\lambda_{\text{low}}}^{\lambda_{\text{high}}} \frac{\Delta\lambda_w \, d\lambda}{(\lambda - \lambda_0 - \Delta\lambda_s)^2 + (\Delta\lambda_w)^2} \quad (31)$$

Results of Numerical Calculations

A computer program to determine the equilibrium composition of, and the total radiated power from multielement metallic plasmas was utilized in the calculations for pure iron, type 304 stainless steel, pure aluminum, and type 2024 and type 6061 aluminum alloy plasmas. Since the numerical calculations for pure iron and type 304 stainless-steel plasmas essentially confirm the results obtained by Harwell, Reid, and Hughes,[1] only the results of the numerical calculations for pure aluminum and aluminum alloy plasmas are presented here. Numerical calculations were carried out over a range of pressures from 1.0–100 atm and temperatures from 5000°K-40,000 °K. For illustrative purposes, only typical data for plasmas at a pressure of 10 atm are presented. The numerical results are qualitatively similar for the other pressures and lead to the same interpretation of the data. In some cases discussed, it is necessary to present the results for a given temperature and pressure. In those cases, the numerical results are presented for a temperature of 10,000 °K. The results are qualitatively the same at the other temperatures considered, even though the magnitude of radiated power in given spectral wavelength bands varied by a considerable amount.

Pure Aluminum Plasma

Numerical calculations were carried out for a pure aluminum plasma consisting of neutral aluminum atoms and the first three ions. The power radiated from a pure aluminum plasma was calculated neglecting spectral line broadening and shift, and then recalculated including these effects. Figures 2a and 3a present the computed results for the 10 atm-10^4 °K case when broadening and line shift were neglected. The radiated power has been summed in 100 Å bands for convenience. The particular wavelength range (4000–8000 Å) was chosen to correspond to the wavelength range and four photomultiplier/filter wavelength intervals (4200–4450 Å, 4600–5050 Å, 5200–5450 Å, and 5570–5980 Å) corresponding to available experimental data.[10] Refer to the discussion of the comparison between theory and experiment for a consideration of the experimental transmission filter behavior with wavelength. It is significant to note in Fig. 2a that the magnitude of the power radiated in the spectral lines is several orders of magnitude larger than the continuum radiation in the wavelength intervals containing any spectral lines. However, only a very few spectral lines for which data are available (Table 1) contribute to the radiation in the wavelength intervals of the experiments. For the case of no broadening and shift, the radiation would appear to be all continuum radiation in the wavelength range 4000–6000 Å. The total power radiated in each of the photomultiplier/filter wavelength intervals of Table I is presented in Fig. 3a as a function of wavelength and temperature for a pressure of 10 atm. Similar data for the case when broadening and shift were included in the calculations is presented in Fig. 3b. The various wavelength intervals are connected by straight lines not to indicate radiation variation between the various intervals but merely to connect the common temperature values.

The effects of line broadening and shift on the spectral distribution are evident when a comparison is made between Figs. 3a and 3b. The power radiated in the various intervals of Fig. 3a is all continuum. From the computer output data[11] it can be determined that there are no shifted line centers in the intervals of interest, but that the power radiated in the "wings" of the broadened spectral lines (Al I lines 3944 and 3461 Å) is sufficient to increase the power radiated in the interval centered at 4325 Å by two orders of magnitude. This increase is in the necessary direction but is insufficient to explain the previous lack of agreement between theory and experimental data.[1] There are less dramatic increases in the intervals centered at 4825 Å, 5325 Å, and 5775 Å. Broadening and shift data for all of the aluminum spectral lines were not available, and only those lines for which data were available in Griem[6] were included in the numerical model. Since the inclusion of the effects of broadening and shift is insufficient to explain the lack of agreement between theory and experiment, it was necessary to include the effects of impurities or elements other than aluminum in the materials used in the experiments.

Multielement Aluminum Alloy (2024) Plasma

A five-element model containing 91% aluminum, 5% copper, 2% magnesium, 1% silicon, and 1% manganese was chosen as

Table 1 Filter/detector wavelength intervals

Filter/detector	Wavelength range (Å)	Center wavelength (Å)
1	4200–4450	4325
2	3820–4930	4375
3	4600–5050	4825
4	4250–5950	5100
5	5200–5450	5325
6	5570–5980	5775
7	3820–7950	5885
8	5950–7950	6950

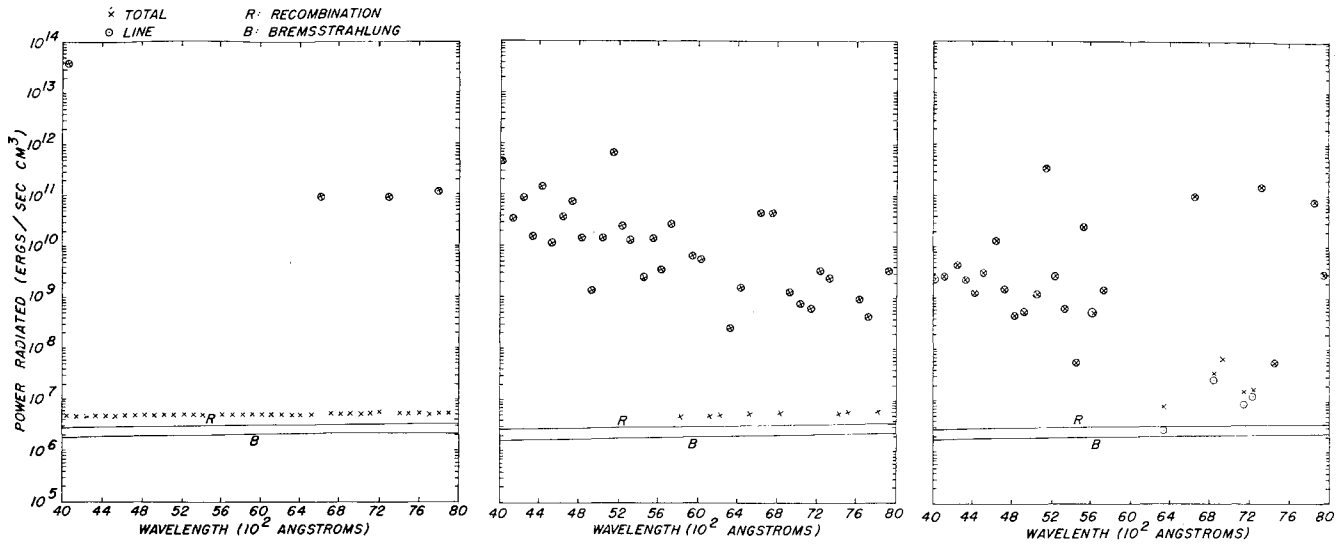

Fig. 2 Power radiated in 100 Å wavelength intervals at a pressure of 10 atm and a temperature of 10,000 °K (neglecting broadening and shift): a) pure aluminum, b) 2024 aluminum plasma, and c) 6061 aluminum plasma.

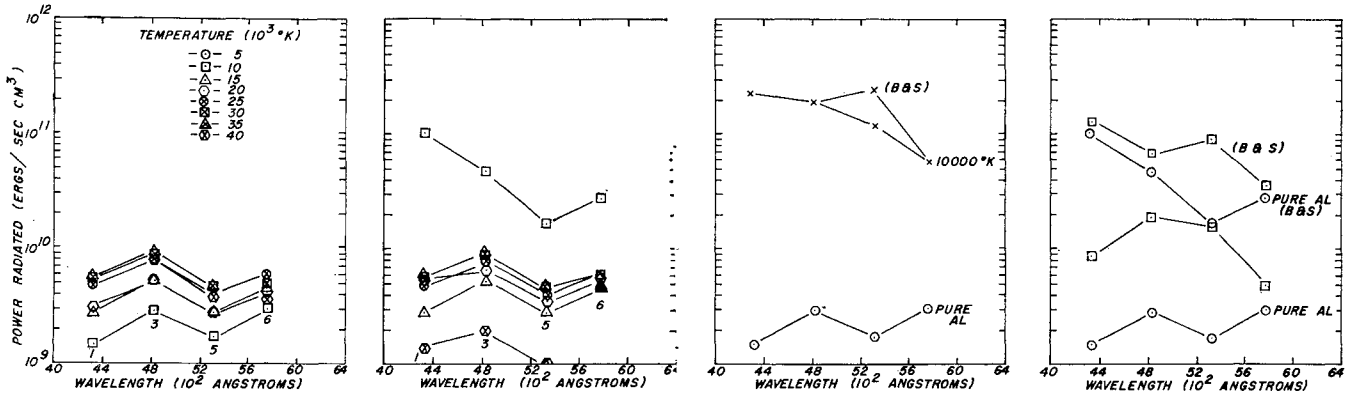

Fig. 3 Total power radiated in four wavelengths bands at 10 atm pressure: a) Pure aluminum (neglecting broadening and shift), b) pure aluminum (including broadening and shift), c) 2024 aluminum, and d) 6061 aluminum.

representative of the type 2024 aluminum alloy used in the experiments.[10] Each of the elements was assumed to have five species (neutral atom through the fourth stage of ionization) except aluminum and copper which had four and three, respectively. The spectral distribution of the radiated power is presented in Fig. 2b when the effects of broadening and shift were neglected. The total power radiated in the four experimental photomultiplier/filter intervals is presented in Fig. 3c. Data for handling the broadening and shift of copper and manganese lines were not available, so that the computations included only the shift and broadening of aluminum, magnesium, and silicon.

When the results for the type 2024 aluminum plasma (Fig. 3c) are compared with the results for the pure aluminum plasma, it is evident that the effect of impurities (inclusion of copper magnesium, silicon, and manganese) is to increase the power radiated by approximately two orders of magnitude over that for pure aluminum in the wavelength intervals centered at 4325 Å, 4825 Å, and 5325 Å. In the interval centered at 5775 Å, the power is increased by about one order of magnitude. In addition to an increase in the radiated power, the relative power radiated in the four intervals is altered so that the "shape" of the spectral distribution curve is no longer the same.

The effect of line broadening and shift is to increase the radiated power in the wavelength interval centered at 5325 Å, whereas the radiation in the other intervals in virtually unchanged from that of the 2024 alloy when the effects of broadening and shift were neglected.

Multielement Aluminum Alloy (6061) Plasma

A five-element model containing 97.3% aluminum, 1.2% magnesium, 0.8% silicon, 0.4% chromium, and 0.4% copper was chosen as representative of type 6061 aluminum used in part of the experiments.[10] Aluminum, magnesium, silicon, chromium, and copper were assumed to have three, four, four, five, and two stages of ionization, respectively.

The spectral distribution of the radiated power is presented in Fig. 2c for the case when line broadening and shift are neglected. The total power radiated in the four photomultiplier/filter wavelength intervals is presented in Fig. 3d for the same conditions as Fig. 2c.

The effects of impurities (constituents other than aluminum) may be observed in two different ways. First, consider the effect of impurity radiation when the effects of line shift and broadening are neglected. The effect of the impurity radiation is to increase the magnitude of the radiation in the bands centered at 4325 Å, 4825 Å, and 5325 Å, whereas that in the band at 5775 Å is increased only slightly. The shape of the spectral distribution curve is changed from an "s" curve to a shape possessing a peak at 4825 Å. Radiation from the alloy differs from that of pure aluminum, since chromium has a multitude of spectral lines which contribute to the various bands. In addition, a small contribution is made by a few copper lines. The radiation from the impurity elements is sufficient to alter the distribution, since the radiation from pure aluminum is essentially all continuum radiation in the four wavelength intervals of Fig. 3a.

Impurity radiation effects can also be seen by comparing the results of the calculations for pure aluminum and the aluminum alloy when the effects of broadening and shift are included. A comparison of the two curves labeled "B&S" in Fig. 3d indicates that the power radiated in the wavelength bands centered at 4325 Å, 4825 Å, and 5775 Å increases very slightly while the power radiated in the band centered at 5325 Å increases by a factor of approximately five. This increase in power can be attributed primarily to the radiation in one magnesium spectral line which has its unshifted line center at 5184 Å.

The effects of line broadening and line shift on the radiation from the 6061 aluminum plasma can be determined from a comparison of the curves of Fig. 3d. A careful study of the computer output data[11] indicates that the gross differences between the pure aluminum ("Pure Al B&S") and the 6061 aluminum ("6061 B&S") curves in Fig. 3d result from the broadening and shift of just one magnesium line. A very intense magnesium line with its unshifted line center at 5184 Å, which was not included in either of the wavelength intervals centered at 4825 Å and 5325 Å, now has its line center wavelength shifted to 5195 Å which is only 5 Å below the lower wavelength limit of the interval centered at 5325 Å. Because of the broadening, this spectral line now makes a large contribution to the radiated power in the interval centered at 5325 Å.

Comparison of Theory and Previous Experiments

Typical experimental results obtained by Hull[10] for 2024 aluminum projectiles impacting 6061 aluminum targets are presented in Fig. 4 for various times after impact. As stated in an earlier study,[1] only the spectral distribution has any meaning in the comparison between theory and experiment since the mathematical model predicts the power radiated from a unit volume of plasma. Unfortunately, the experimental data were obtained prior to the beginning of theoretical study of Harwell, Reid, and Hughes,[1] so that there was no way to determine the radiating volume of the experimental plasma source.

Another problem in making a meaningful comparison between the theoretical calculations and the available experimental data is the manner which the experimental data[10] were corrected for photomultiplier response and filter attenuation of the emitted radiation. The experimental data were reported after the filter response correction had been made. Unfortunately, the response factors were assumed to be flat-topped with a sharp cutoff at the wavelength edges of the transmission region. However, it is known that there was some radiated power transmitted in the wings of the filter bands; e.g., the filter for the wavelength interval 4200–4450 Å transmitted some radiation in the wavelength region below 4100 Å. Since the radiation at the wavelengths 3944 Å is many orders of magnitude larger than from other known lines, even a small transmission factor of the filter would allow a considerable amount of the radiation to be detected by the photomultiplier. Since the photomultiplier/filter response curves were available but the experimental measurements and calculations were not, it was decided to apply the transmission filter factors to the theoretical data so that a meaningful comparison could be made.

A comparison between the theoretical calculations of an aluminum plasma and a 6061 aluminum alloy plasma with and without the effects of broadening and shift and the experimental results can be made by referring to Fig. 5. First, compare the calculated results for a pure aluminum plasma with the experimental results presented in Fig. 4. The pure aluminum results have been multiplied by a factor of ten to permit ease of comparison. There is a notable lack of agreement between the experimental results and the results calculated for a pure aluminum plasma.

Next, compare the results for a pure aluminum plasma which include the effects of broadening and shift (the curve labeled "Pure Al B&S"). The results qualitatively agree somewhat for the wavelength intervals centered at 4325 Å, 4825 Å, and 5775 Å. This improvement in agreement is explained primarily by the inclusion of radiation from the 3944 Å and 3961 Å broadened lines of Al I. However, there is still a definite lack of agreement for the wavelength interval centered at 5325 Å.

As expected, the results computed for the 6061 aluminum alloy when the effects of broadening and shift were neglected (the curve labeled "6061 Al" in Fig. 5) do not compare favorably with the experimental results.

Finally, calculations were carried out for the 6061 aluminum alloy in which the effects of line broadening and shift were included (refer to the curve labeled "6061 Al B&S"). An attempt was then made to determine whether similar curves could be found in the experimental data that agreed qualitatively with the theoretical results. As shown by the curve labeled "Experimental" in Fig. 5, curves of similar shape could be found in both the theoretical and experimental results. In general, curves of spectral distribution, at specified temperature and pressure, can be selected from the

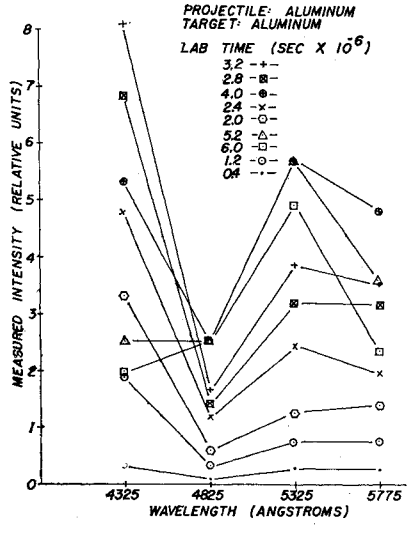

Fig. 4 Typical experimental data for aluminum-aluminum impacts.

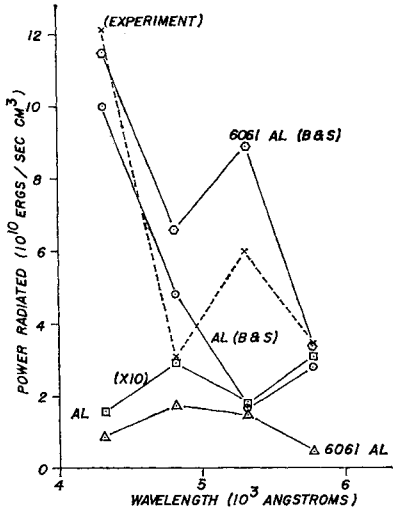

Fig. 5 Comparison of theoretical power radiated from pure aluminum and 6061 aluminum alloy at 10 atm, 10^4 °K with and without broadening and shift and the experimental data.

theoretical results that agree qualitatively with the temporal behavior observed in the experiments. A more detailed knowledge of the experimental conditions will be required before a more definitive qualitative agreement can be achieved.

Conclusions

A theoretical model which represents the hypervelocity impact flash as radiation from multielement metallic plasmas has been developed. Calculations were performed for five element representations of type 2024 and type 6061 aluminum alloy impact plasmas. The effects of line broadening and shift were included in the calculations.

In order to obtain qualitative agreement theory and experiment, it was necessary to include both the impurity effects and the line broadening and shift effects. This study demonstrated that the radiation emitted by a transient impact gas cloud can be represented as radiation from a high-pressure metallic plasma.

It was found that if the pure metallic gas has no strong spectral lines in a given wavelength band, the power radiated will be extremely sensitive to the addition of a few strongly radiating impurities. For example, the radiation from a 6061 aluminum alloy plasma in one wavelength interval was significantly increased because of the presence of a single strong magnesium spectral line in that interval. In the case of aluminum projectiles, it would be possible to enhance the emitted radiation by the addition of a seed material with a few strong spectral lines which are easy to identify. Such seed materials could be, for example, magnesium, cadmium,[12] cesium, or other strong line-radiating elements. Such radiation enhancement could lead to a significant increase in remote impact detection ability. The addition of other seed materials could lead to a reduction of radiation which might be of interest in some applications.

Additional research will be necessary before the calculations can be easily reversed to yield the pressure, temperature, and the physical properties of an unknown projectile-target combination from a knowledge of only the radiated power.

References

[1] Harwell, K. E., Reid, J. L., and Hughes, A. R., "Calculated Equilibrium Composition and Radiation of Metallic Plasmas Produced in Hypervelocity Impact," *Journal of Spacecraft and Rockets*, Vol. 8, No. 4, April 1971, pp. 358–366.

[2] Jean, B. and Rollins, T., "Hypervelocity Impact Flash for Hit Detection and Damage Assessment," TR AFATL-TR-68-46, 1968, Air Force Armament Lab., Eglin Air Force Base, Fla.

[3] Jean, B., "Experimental Observations of Optical Radiation Associated with Hypervelocity Impact," *AIAA Journal*, Vol. 4, No. 10, Oct. 1966, pp. 1854–1856.

[4] Jean, B. and Rollins, T. L., "Radiation from Hypervelocity Impact Generated Plasma," *AIAA Journal*, Vol. 8, No. 10, Oct. 1970, pp. 1742–1748.

[5] Griem, H. R., "Validity of Local Thermal Equilibrium in Plasma Spectroscopy," *Physical Review*, Vol. 131, No. 3, 1963, pp. 1170–1176.

[6] Griem, H. R., *Plasma Spectroscopy*, McGraw-Hill, New York, 1964.

[7] McWhirter, R. W. P., "Spectral Intensities," *Plasma Diagnostic Techniques*, edited by R. H. Huddlestone and S. L. Leonard, Academic Press, New York, 1965, pp. 201–264.

[8] Drellishak, K. S., Knapp, C. F., and Cambel, A. B., "Partition Function and Thermodynamic Properties of Argon Plasma, *The Physics of Fluids*, Vol. 6, No. 9, Sept. 1963, pp. 2180–1288.

[9] Olsen, H. N., "Partition Function Cut-Off and Lowering of the Ionization Potential in Argon Plasma," *Physical Review*, Vol. 124, 1961, p. 1703.

[10] Reid, J. L., Harwell, K. E., and Hughes, A. R., "Theoretical and Experimental Investigation of the Relationship of Impact Flash to Physical Damage," TR AFATL-TR-67-138, 1967, Air Force Armament Lab., Eglin Air Force Base, Fla.

[11] Harwell, K. E., "Hypervelocity Impact Flash Radiation Model," TR AFATL-TR-69-100, 1969, Air Force Armament Lab., Eglin Air Force Base, Fla.

[12] McCay, T. D., "Equilibrium Radiation from a High Temperature Pure Cadmium Plasma," Master of Science thesis, Dec. 1969, Aerospace Engineering Dept., Auburn Univ., Auburn, Ala.